Faraday Discussions

Cite this: *Faraday Discuss.*, 2025, **255**, 495

PAPER

Probing assembly/disassembly of ordered molecular hydrogels†

Susana M. Ramalhete,[a] Karol P. Nartowski, ‡[ab] Hayley Green,[c] Jesús Angulo, [d] Dinu Iuga, [e] László Fábián, [a] Gareth O. Lloyd *[f] and Yaroslav Z. Khimyak *[ab]

Received 24th April 2024, Accepted 17th May 2024
DOI: 10.1039/d4fd00081a

Supramolecular hydrogels have a wide range of applications in the biomedical field, acting as scaffolds for cell culture, matrices for tissue engineering and vehicles for drug delivery. L-Phenylalanine (Phe) is a natural amino acid that plays a significant role in several physiological and pathophysiological processes (phenylketonuria and assembly of fibrils linked to tissue damage). Since Myerson *et al.* [*Chem. Eng. Commun.*, 2002, **189**(8), 1079–1090] reported that Phe forms a fibrous network *in vitro*, Phe's self-assembly processes in water have been thoroughly investigated. We have reported structural control over gelation by introduction of a halogen atom in the aromatic ring of Phe, driving changes in the packing motifs, and therefore, dictating gelation functionality. The additional level of control gained over supramolecular gelation *via* the preparation of multi-component gel systems offers significant advantages in tuning functional properties of such materials. Gaining molecular-level information on the distribution of gelators between the inherent structural and dynamic heterogeneities of these materials remains a considerable challenge. Using multicomponent gels based on Phe and amino-L-phenylalanine (NH_2-Phe), we will explore the patterns of ordered/disordered domains in the gel fibres and will attempt to come up with general trends of interactions in the gel fibres and at the fibre/solution interfaces. Phe and NH_2-Phe were found to self-assemble in water into crystalline hydrogels. The determined faster dynamics of exchange between the gel and solution states of NH_2-Phe in comparison

[a]*School of Pharmacy, University of East Anglia, Norwich Research Park, Norwich, NR2 1TS, UK. E-mail: Y. Khimyak@uea.ac.uk*

[b]*Department of Drug Form Technology, Wroclaw Medical University, Borowska 211A, 50-556 Wroclaw, Poland*

[c]*Institute of Chemical Sciences, School of Engineering and Physical Sciences, Heriot-Watt University, Edinburgh, EH14 4AS, UK*

[d]*Instituto de Investigaciones Químicas (CSIC-US), Avda. Américo Vespucio, 49, Sevilla 41092, Spain*

[e]*Department of Physics, University of Warwick, Coventry, CV4 7AL, UK*

[f]*School of Chemistry, University of Lincoln, Lincoln, LN6 7DL, UK. E-mail: GLloyd@lincoln.ac.uk*

† Electronic supplementary information (ESI) available: Additional experimental data, structural characterisation of hydrogels including single and powder X-ray diffraction data, NMR spectra recorded in solution and solid state, and data of thermal analysis. CCDC 2350191. For ESI and crystallographic data in CIF or other electronic format see DOI: https://doi.org/10.1039/d4fd00081a

‡ Deceased author.

with Phe were correlated with weaker intermolecular interactions, highlighting the role of head groups in dictating the strength of intermolecular interactions. In the mixed Phe/NH_2-Phe systems, at a low concentration of NH_2-Phe, disruption of the network was promoted by interference of the aliphatics of NH_2-Phe with the electrostatic interactions between Phe molecules. At high concentrations of NH_2-Phe, multiple-gelator hydrogels were formed with crystal habits different from those of the pure gel fibres. NMR crystallography approaches combining the strengths of solid- and solution-state NMR proved particularly suitable to obtain structural and dynamic insights into the "ordered" fibres, solution phase and fibre/solution interfaces in these gels. These findings are supported by a plethora of experimental (diffraction, rheology, microscopy and thermal analysis) and computational methods.

Introduction

Supramolecular gels are colloidal dispersions formed by a rigid three-dimensional structure.[1] They possess solid-like rheological properties, despite their high contents of solvent.[1] The building blocks of supramolecular gels that have a molecular weight of less than 1000 Da are referred to as low-molecular-weight (LMW) gelators.[2] Their self-assembly occurs through unidirectional non-covalent forces, leading to formation of entangled fibrillar networks that arrest the solvent *via* surface tension and capillary forces.[3,4] The resulting gels are stimuli responsive due to the reversible nature of the interactions, so external stimuli can prompt gel-to-solution transitions, a change of shape or release of entrapped molecules.[5] This feature is behind their broad range of biomedical applications, with them being developed as scaffolds for tissue engineering,[6] matrices for cellular growth[7] or vehicles for advanced drug delivery.[6–8] The design and discovery of novel structures capable of gelling in a variety of solvents has been of great interest due to their unparalleled properties as soft materials.

Multi-component gel systems are composed of two or more molecules.[9,10] They can form gels only when combined, gel independently (Fig. 1a), or have their properties modified in the presence of non-gelling additives (Fig. 1b).[9] When both

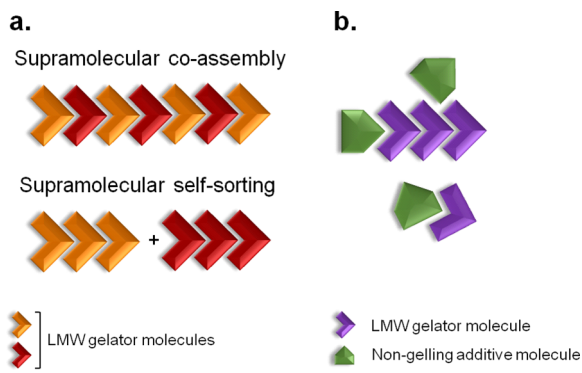

Fig. 1 Two-component self-association. (a) Supramolecular co-assembly and self-sorting processes can occur when both molecules are LMW gelators. (b) When the additive is a non-gelling molecule, the physical properties of the resulting gel material might be modified. Adapted from ref. 9.

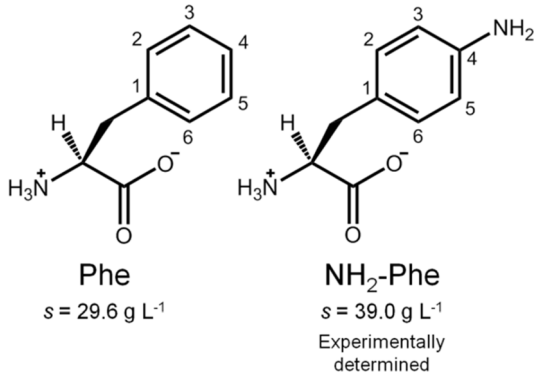

Fig. 2 Molecular structures of zwitterionic Phe and NH_2-Phe and their water solubilities at 298 K.

molecules form gel networks on their own, the resulting mixed system may be formed by interpenetrated structures of the pure gelators, termed self-sorting, or might give rise to new mixed architectures, a process designated as co-assembly (Fig. 1a).[9] Understanding, at the molecular level, the structure of multi-component gels provides opportunities to design customised soft materials.

Phenylketonuria is an autosomal recessive disease that originates from mutations in the gene coding for phenylalanine hydroxylase.[11,12] The absence of this enzyme leads to large accumulation of L-phenylalanine (Phe) in the plasma, brain tissue and cerebral fluids.[11] The resultant accumulation of Phe leads to formation of stable toxic aggregates, which have been detected at micromolar concentrations *in vivo*.[11–13] It has also been determined previously that Phe self-assembles into long fibres that give rise to a supramolecular crystalline hydrogel at millimolar concentrations *in vitro*.[11,13–16]

In this report, we discuss our findings on amino-L-phenylalanine (NH_2-Phe) and its solution- and solid-state interactions with Phe (Fig. 2). The main purpose of this research project was to study single and multi-component hydrogels of Phe and NH_2-Phe, and to pinpoint the interactions responsible for the disruption of Phe hydrogels upon the addition of NH_2-Phe. Hence, the present study describes the mechanism of disruption of Phe hydrogels upon adding low concentrations of NH_2-Phe, and how this information provides an insight into the structure and dynamics of single- and multiple-gelator hydrogels (which are formed at high concentrations of NH_2-Phe). The resulting materials were characterised using microscopy, rheology, diffraction and advanced nuclear magnetic resonance (NMR) spectroscopy, methodologies that are able to probe different regimes of mobility, levels of self-organisation and intermolecular connectivities.

Results and discussion

Macroscopic and morphological characterisation

When Phe and NH_2-Phe were mixed in water, different products were obtained depending on the concentration and molar ratio of the gelator molecules (Fig. 3 and 4). A detailed description of the concentration and molar ratio of hydrogels

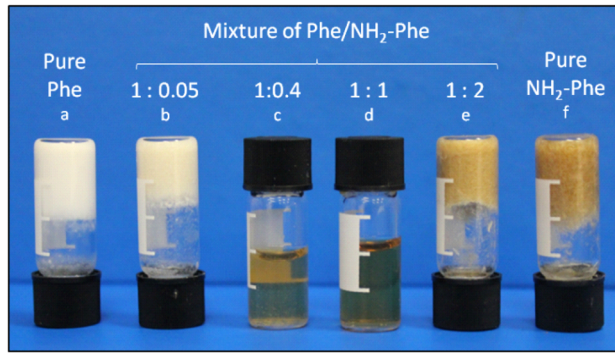

Fig. 3 Images of hydrogels of (a) Phe (303 mM), (b) Phe/NH_2-Phe (1 : 0.05), (e) Phe/NH_2-Phe (1 : 2) and (f) NH_2-Phe (606 mM), (c) the suspension of Phe/NH_2-Phe (1 : 0.4) and (d) the solution of Phe/NH_2-Phe (1 : 1).

under study can be found in the ESI (Table S1†). For comparison purposes, the concentration of Phe was maintained at 303 mM, which corresponds to the concentration at which the pure monohydrate form of Phe is obtained.[16]

Phe gives rise to white opaque hydrogels (Fig. 3a), composed of long hair-like fibres (Fig. 5a), at concentrations higher than 212 mM.[16] When small concentrations of NH_2-Phe were added (up to 1 : 0.2), a brownish colouration appeared, but the self-sustaining properties of the material were kept (Fig. 3b). Between the ratios of 1 : 0.2 and 1 : 0.4, a heterogeneous sample was obtained, containing white bulky clouds in suspension. These samples exhibited flow when inverted. When the concentration of NH_2-Phe was increased further, thin white particles

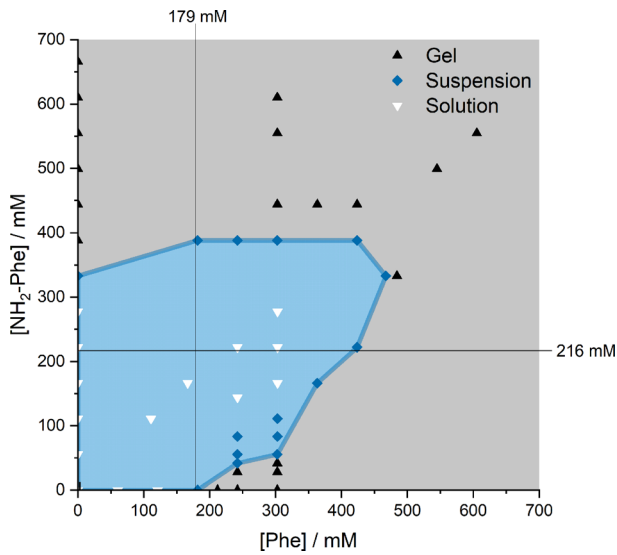

Fig. 4 Phase diagram of the products obtained depending on the concentration and molar ratio of Phe and NH_2-Phe in water. The water solubilities of Phe (179 mM) and NH_2-Phe (216 mM) are highlighted with black lines.

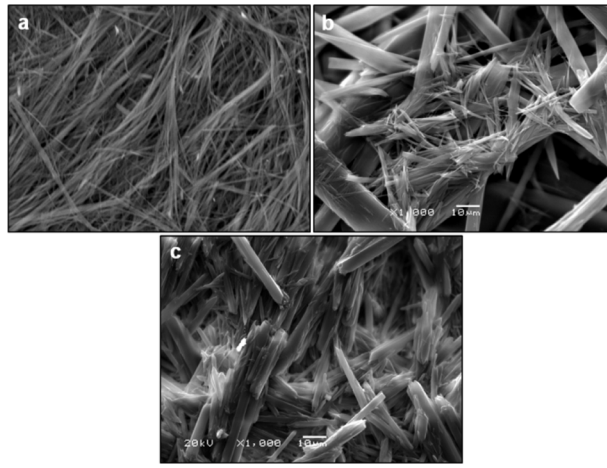

Fig. 5 SEM images of (a) Phe (303 mM), (b) Phe/NH_2-Phe (1 : 2) and (c) NH_2-Phe (606 mM) dried hydrogels. The hair-like fibres of Phe had an average width of 1.1 μm (ranging between 0.4 and 1.7 μm), whereas the average width of the needle-like fibres of NH_2-Phe was 25.3 μm (ranging between 2.6 and 47.9 μm).

were observed in suspension (Fig. 3c). Above a 1 : 1 ratio, these particles were fully solubilised and a clear brown solution was obtained (Fig. 3d). When both molecules were mixed above their individual critical gelation concentrations (CGC) (CGC_{Phe} = 212 mM and $CGC_{NH_2\text{-}Phe}$ = 388 mM), brown hydrogels containing white crystalline structures were formed (Fig. 3e and 5b). The white elements were attributed to the long hair-like fibres belonging to Phe, interpenetrated with shorter and thicker needle-like crystals belonging to NH_2-Phe (Fig. 5b). The presence of distinguishable morphologies is commonly associated with self-sorted materials, composed of intertwined fibres of the pure hydrogels.[9]

Throughout these studies, we discovered that NH_2-Phe is also able to self-assemble in water into organised structures, forming brown opaque crystalline hydrogels (Fig. 3f) composed of wide needle-like fibres (Fig. 5c) at concentrations above 388 mM. The gelation process of NH_2-Phe was found to be very dependent on quenching and agitation rates. Gel materials were successfully obtained only when the hot solutions were immediately cooled down in an ice bath with constant agitation, as slow cooling rates and lack of agitation favoured precipitation of crystalline needle-like components over gel formation. The three-dimensional habit of these needles corresponded to the crystal structure of the NH_2-Phe gel fibres.

Mechanical properties of hydrogels

With the goal of understanding the consequences of combining Phe and NH_2-Phe, we investigated initially how the mechanical properties of these crystalline gels were modulated. The strength of the hydrogel fibres was assessed by determining the materials' viscoelastic parameters during frequency-sweep studies. The phase angle (δ) formed between the phases of stress and strain was below 10° for pure hydrogels, reflecting the solid-like nature of these materials.[17] The

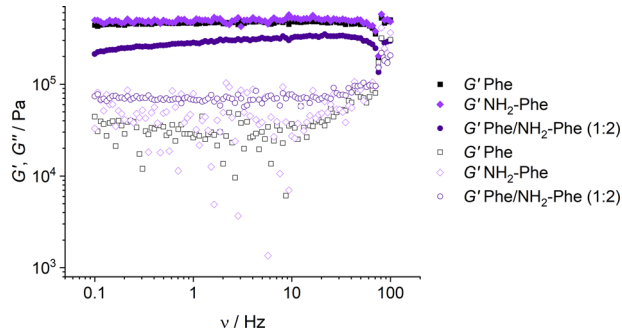

Fig. 6 Storage (G') and loss (G'') moduli for Phe (303 mM), Phe/NH_2-Phe (1 : 2) and NH_2-Phe (606 mM) hydrogels in frequency-sweep experiments.

storage moduli (G') for Phe and NH_2-Phe hydrogels were on the order of 10^5 Pa ($G'_{Phe} = 4.7 \times 10^5$ Pa and $G'_{NH_2\text{-}Phe} = 5.1 \times 10^5$ Pa) and these values were one order of magnitude greater than the loss moduli (G'') ($G''_{Phe} = 3.2 \times 10^4$ Pa and $G''_{NH_2\text{-}Phe} = 3.1 \times 10^4$ Pa) (Fig. 6), characteristic values of robust gels.[18] These results confirmed the viscoelastic nature of the materials.

Interestingly, weaker gel fibres with lower resistance to deformation were found for the mixed hydrogel Phe/NH_2-Phe (1 : 2). The higher values of the phase angle ($\delta > 10$) in combination with the lower elastic response ($G'_{Phe/NH_2\text{-}Phe} = 2.7 \times 10^5$) and the higher inelastic response ($G''_{Phe/NH_2\text{-}Phe} = 7.1 \times 10^4$ Pa) for these hydrogels compared to the pure materials pointed towards a system showing less elastic behaviour. These variations in the bulk properties of the pure and mixed gels reflected differences in their molecular and supramolecular level arrangements.

Characterisation of the structure of the gel fibres

The identification of diffraction peaks in the powder X-ray diffraction (PXRD) patterns of the hydrogels (Fig. 8) confirmed their crystalline nature. Phe hydrogel fibres are composed of the Phe monohydrate, as identified in our previous studies using single X-ray diffraction and corroborated with solid-state NMR and DFT calculations.[16] Using single-crystal and powder X-ray diffraction experiments (Fig. S12‡), the crystal structure of the NH_2-Phe gel fibres was determined successfully (Fig. 7 shows the packing of the structure as determined by single-crystal diffraction). It is clear that the Phe monohydrate and the $(NH_2\text{-}Phe)_2(H_2O)_3$ structures are not isostructural and therefore should not easily form solid solutions, according to the Kitaigorodsky studies and design rules for solid solutions.[19–25] This is important to note here and will be discussed further in the manuscript. What follows is a description of the NH_2-Phe crystal form and the structural similarities to the Phe monohydrate structure.

The structure determined from samples of NH_2-Phe in water was ascertained to be a NH_2-Phe hydrate [the stoichiometry of the asymmetric unit is $(NH_2\text{-}Phe)_2(H_2O)_3$]. The structure of the gel fibres of the Phe gels has a crystallographic stoichiometry of $(Phe)_2(H_2O)_2$, from the asymmetric unit. The "extra hydration" of the NH_2-Phe hydrate is not unexpected, as the amino group provides both

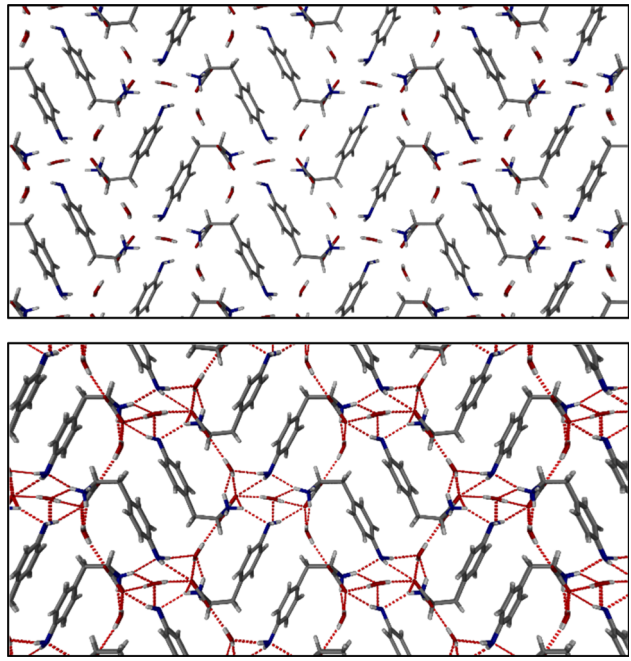

Fig. 7 Molecular packing of NH_2-Phe shown along the *a* axis.

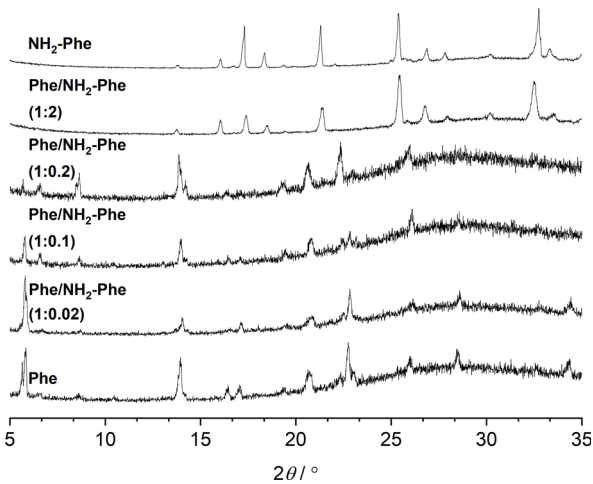

Fig. 8 PXRD patterns of Phe (303 mM), Phe/NH_2-Phe (1 : 0.02), Phe/NH_2-Phe (1 : 0.1), Phe/NH_2-Phe (1 : 0.2), Phe/NH_2-Phe (1 : 2) and NH_2-Phe (606 mM) hydrogels.

hydrogen-bond donation and acceptor character, but these components are not stoichiometric. The amino groups of both molecules in the asymmetric unit only interact with water as a donor hydrogen-bond group (the amino groups also donate hydrogen bonding to the carboxylate groups), with the acceptor hydrogen-bonding property of the amino groups interacting with the ammonium group

only, and not water. To better understand the interactions of NH_2-Phe within the crystal structure, we turned to the determination of not only the hydrogen bonding, but estimates of the interaction energies.[26–29]

Interaction maps of Phe and NH_2-Phe were calculated to determine if there was a preferential direction associated with intermolecular interactions. This preferred-direction hypothesis has been utilised by a number of researchers to understand the relationship between crystal structures and gelation/fibre formation.[3,30–33] Both single crystal structures' hydrogen positions were normalised using Mercury (CCDC). The Crystallographic Information Files (CIFs) were then analysed utilising the Crystal Explorer software and Tonto. The Phe structure reveals a strong unidirectional preference for the dimer of Phe molecules. The dimers interact through a total interaction energy of 168.1 kJ mol^{-1}, but this dimer interaction does not form a periodic pattern. However, the two molecules in the asymmetric unit strongly interact with each other through directional periodic interactions (along the *b* axis) of 125.3 and 125.5 kJ mol^{-1}. These interaction strengths are a combination of zwitterion-based ionic interactions and charge-assisted hydrogen bonds, as we and others have determined previously.[16] Although the preference of the interactions is not as large in the $(NH_2\text{-Phe})_2(H_2O)_3$ structure, there is still some degree of directional preference. The stacking of the NH_2-Phe zwitterions is still clearly visible and dominant, with calculated interaction energies of 115.6 kJ mol^{-1} and 110.1 kJ mol^{-1} for the two molecules in the asymmetric unit. These interactions are directed along the *a* axis and were found to be the strongest interaction between neighbouring NH_2-Phe molecules. The next-strongest interactions are more than 20 kJ mol^{-1} weaker, are associated with the hydrogen bonding between the amine groups and the zwitterion end group, and are found perpendicular to the stronger interactions. The next-strongest interactions (*ca.* 50 kJ mol^{-1}) are associated with water hydrogen bonding. What these calculations highlight is that the one-dimensional hypothesis often utilised in connecting gelation with crystal forms can be applied here as well, even though the hydrogen bonding and π–π interactions do not clearly show a preferential direction (the point of the energy framework analysis). Coupling these interactions with the Bravais–Friedel–Donnay–Harker (BFDH) morphology prediction (performed in the CSD Mercury program), we can clearly see how the fibrous material is generated through the intermolecular interactions of NH_2-Phe, in association with water.

The addition of low amounts of NH_2-Phe to the Phe hydrogels did not affect the three-dimensional molecular arrangement of the Phe gel fibres, as the PXRD patterns (Fig. 8) and ^1H–^{13}C CP/MAS NMR spectra (Fig. 9) were identical to those of pure Phe. The crystalline structures of particles in suspension – Phe/NH_2-Phe (1 : 0.4) – also matched the monohydrate form of Phe. However, a further increase in the concentration of NH_2-Phe led to different results. The PXRD pattern of the mixed hydrogel was very similar to the one of pure NH_2-Phe (Fig. 8), suggesting an analogous supramolecular arrangement. This is not surprising, as NH_2-Phe is present at a higher concentration, imposing its crystalline organisation.

To help interpret the observed differences, the structure of the rigid components of the fibres was assessed using ^1H–^{13}C CP/MAS solid-state NMR spectroscopy. This method relies on the efficient transfer of polarisation from ^1H to strongly dipolar-coupled ^{13}C nuclei,[34] and only the rigid gel fibres satisfy this condition. ^1H–^{13}C CP/MAS NMR spectra of Phe hydrogels showed the

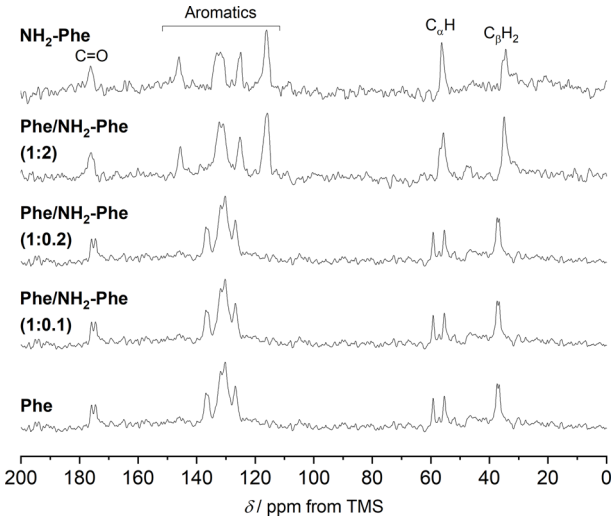

Fig. 9 $^{1}H-^{13}C$ CP/MAS NMR spectra of Phe (303 mM), Phe/NH_2-Phe (1 : 0.1), Phe/NH_2-Phe (1 : 0.2), Phe/NH_2-Phe (1 : 2) and NH_2-Phe (606 mM) hydrogels acquired with an MAS rate of 8.5 kHz using a 400 MHz solid-state NMR spectrometer.

characteristic peak splitting of the monohydrate form, with two peaks per carbon site (Fig. 9 and 10), corresponding to two non-equivalent magnetic environments. Regarding the NH_2-Phe hydrogel, the very good agreement between the ^{13}C chemical shift values determined experimentally and those predicted using CASTEP for NH_2-Phe hydrogels (Fig. 11) allowed us to confidently confirm the molecular packing motif within the gel fibres.

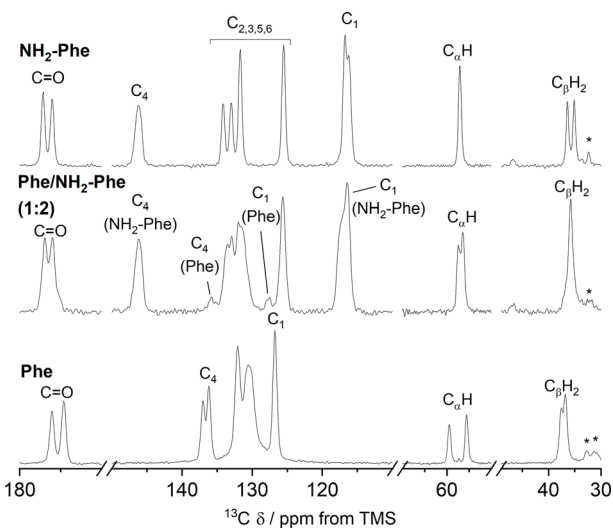

Fig. 10 Amplification of $^{1}H-^{13}C$ CP/MAS NMR spectra of Phe (303 mM), Phe/NH_2-Phe (1 : 2) and NH_2-Phe (606 mM) dry hydrogels acquired with an MAS rate of 10 kHz using a 400 MHz solid-state NMR spectrometer.

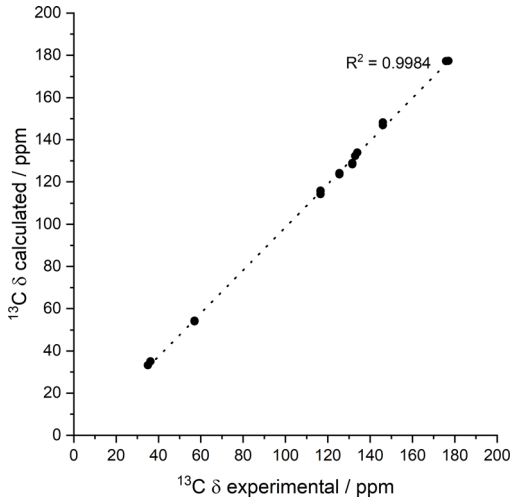

Fig. 11 Experimental ^{13}C chemical shift values for the NH_2-Phe (606 mM) dry hydrogel acquired with an MAS rate of 10 kHz *vs.* calculated values for the predicted structure. Calculated isotropic chemical shieldings were converted to chemical shifts by matching the calculated and observed chemical shift of the peak at 168.25 ppm.

Even though the PXRD pattern of the Phe/NH_2-Phe (1 : 2) hydrogel presented a great resemblance to that of pure NH_2-Phe, differences were identified in the CP/MAS studies (Fig. 10). The ^{1}H–^{13}C CP/MAS NMR spectrum was not a simple superposition of both spectra of the pure hydrogels (Fig. S14†). Instead, chemical shift variation was observed for the carbonyl, aromatic and $C_\beta H_2$ carbons (Table S6†). Moreover, the aromatic carbons of the mixtures were significantly broadened with different line shapes in comparison with the spectra of the single-gelator hydrogels. These studies showed that NH_2-Phe is not imposing its supramolecular organisational preference, as suggested by PXRD data, but both molecules are intricately modifying each other's packing motifs.

^{15}N MAS NMR experiments further supported the previous findings. ^{15}N is an NMR-active nucleus sensitive to changes in the local environments of N-bearing groups and geometry of hydrogen bonds; therefore, it contains specific structural information.[35] Due to its poor NMR sensitivity and negative gyromagnetic ratio,[35] ^{15}N-labelled Phe was used when monitoring the local environment of $^{15}NH_3^+$-motifs in single- and multiple-gelator hydrogels. The high-field ^{1}H–^{15}N CP/MAS spectrum of the Phe hydrogel showed two sharp peaks corresponding to the two molecules per asymmetric unit of the monohydrate form (Fig. 12). Interestingly, ^{15}N-NMR peaks in the spectrum of the mixed gel system were significantly broadened with an additional ^{15}N peak. The differences in peak intensities reflected that these ^{15}N sites were structurally different. Furthermore, the presence of a variety of magnetically non-equivalent environments was consistent with the line broadening observed in the corresponding ^{1}H–^{13}C CP/MAS NMR spectrum, and showed that new $^{15}NH_3^+$-Phe environments were formed within the rigid fibres of multiple-gelator hydrogels. Altogether, these data show that molecules within the supramolecular structures of mixed gel

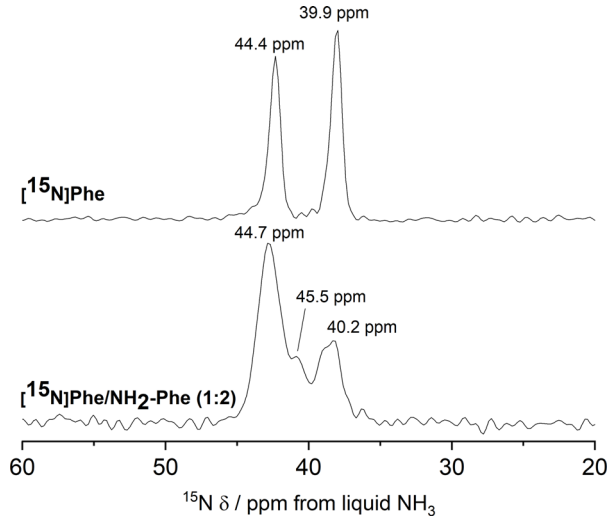

Fig. 12 ^{1}H–^{15}N CP/MAS NMR spectra of ^{15}N-labelled [^{15}N]Phe (303 mM) and [^{15}N]Phe/NH_2-Phe (1 : 2) dried hydrogel samples, acquired with MAS rates of 10 kHz, using an 850 MHz solid-state NMR spectrometer.

systems have different local environments in comparison with those in pure hydrogels.

Investigation of interactions responsible for aggregation

Understanding the dynamics of disruption and identifying the structure of the products may shed light on the composition of the solid-state components that pre-empt multiple-gelator hydrogelation. The supramolecular arrangement of the particles suspended in the Phe/NH_2-Phe (1 : 0.4) mixed system corresponded to the monohydrate form with Phe and NH_2-Phe present in the aggregates in a 1 : 1 ratio (equimolar). Interestingly, when studying spatial correlations between both molecules in the suspension and solution regimes, no cross-peaks were found between Phe and NH_2-Phe in 2D ^{1}H–^{1}H NOESY spectra (Fig. S22†). However, these through-space interactions were detected in the hydrogel samples (Fig. 14), which are characterised by different cross-relaxation and relaxation rates. Hence, it was proposed that the lifetime of these interactions in solution and suspension is too short on the time scale of the experiment, *i.e.*, faster than the cross-relaxation rate.

Identification of intermolecular interactions responsible for network disruption

In solution, gelation and crystallisation have the common starting point of nucleation followed by fibre or crystal growth.[36] These processes affect the local environments of nuclear spins. NMR is sensitive to molecular environments and conformational changes, frequently translated by changes in chemical shifts. Experiments monitoring the chemical shift values of Phe with gradual addition of NH_2-Phe were unsuccessful. Working under gel-forming conditions does not provide a clear trend in the modification of local ^{1}H environments, since the peaks are significantly broadened and correspond to an average of multiple

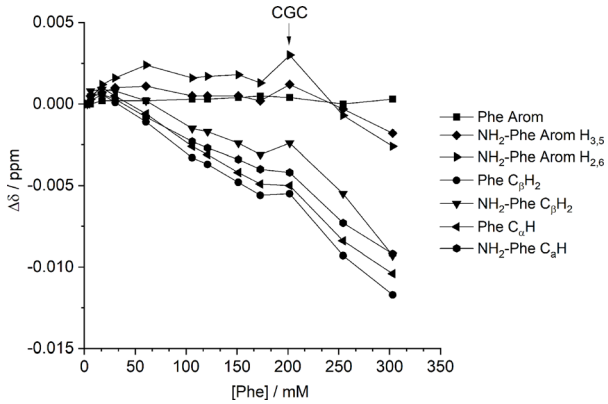

Fig. 13 Chemical shift variation (Δ) in ^{1}H-NMR spectra in dilution studies of the Phe/NH_2-Phe (1 : 0.15) hydrogel, measured at 298 K.

species in both solution and gel states.[37,38] The mechanism of disruption was therefore investigated *via* dilution studies of the Phe/NH_2-Phe (1 : 0.15) hydrogel. Several ^{1}H-NMR spectra were acquired at variable concentration to identify which proton sites were most affected by aggregation processes. The most significant chemical shift variation was observed for the $C_\alpha H$ and $C_\beta H_2$ protons of both Phe and NH_2-Phe (Fig. 13), meaning the aliphatic region of both molecules was the most involved in the formation of intermolecular interactions. These findings also pointed towards participation of NH_2-Phe in pre-gelation aggregation processes.

The dynamic character of supramolecular hydrogels is an advantageous feature, as molecules on the surface of fibres carry information from the network when returning to solution. The phenomenon of solution-state NMR spectra containing information from the hydrogel fibres due to fast molecular exchange between solution and gel states has been described previously.[39,40] Therefore, the network can be investigated indirectly. 2D ^{1}H–^{1}H NOESY NMR experiments were conducted on the Phe/NH_2-Phe (1 : 0.15) hydrogel to determine the interactions responsible for disruption of the network and probable solubilisation of Phe molecules in water. Negative cross-peaks, characteristic of medium-to-large molecules,[41] were observed between all protons (Fig. 14). The resulting map of through-space connectivities allowed calculation of interproton distances (Table 1). In combination with the evolution of nOe enhancements with mixing time (Fig. S22†), interproton distances enabled the conclusion that the most significant interaction was between NH_2-Phe aliphatic protons and Phe $C_\alpha H$. NH_2-Phe and Phe probably interact in solution *via* their electrostatic moieties, suggesting that the mechanism of disruption of Phe dimers[16] occurs *via* mixed H-bonding of the zwitterionic parts.

Characterisation of dynamics of disruption and gel formation

Since ^{1}H-NMR is a quantitative analytical method, it allows the determination of the ratio between molecules dissolved in water and molecules forming a rigid gel network. The latter's short transverse relaxation times, strong dipolar couplings

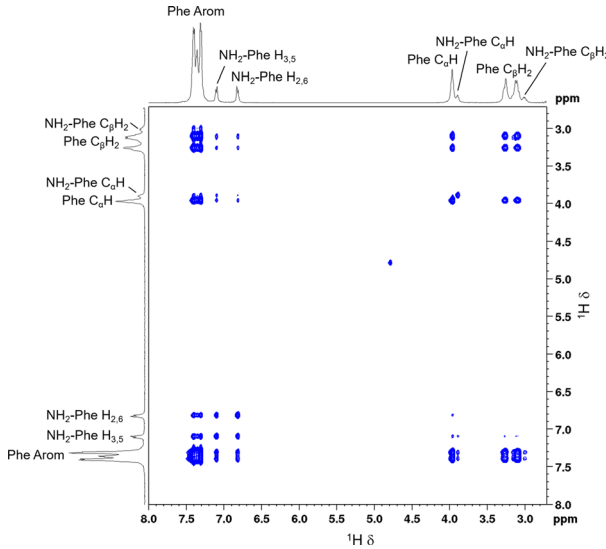

Fig. 14 2D ^{1}H–^{1}H NOESY NMR spectrum of the Phe/NH_2-Phe (1 : 0.15) hydrogel with a mixing time of 0.5 s, measured at 298 K.

Table 1 Inter-proton distances calculated from the 2D ^{1}H–^{1}H NOESY NMR spectrum of the Phe/NH_2-Phe (1 : 0.15) hydrogel with a mixing time 0.01 s, measured at 298 K, using the $H_{2,6}$–$H_{3,5}$ distance from NH_2-Phe as a reference. Average errors of 7% were assumed as for fast-tumbling molecules in viscous solvents[27]

Correlation	r (Å)	Error (Å)
NH_2-Phe Arom $H_{2,6}$: NH_2-Phe Arom $H_{3,5}$	2.28[a]	—
NH_2-Phe $C_\beta H_2$: Phe $C_\beta H_2$	2.48	0.20
NH_2-Phe Arom $H_{3,5}$: Phe Arom $H_{3,5}$	2.68	0.21
NH_2Phe $C_\alpha H$: Phe $C_\beta H_2$	2.70	0.22
NH_2-Phe Arom $H_{3,5}$: Phe Arom $H_{2,6}$	2.80	0.22
NH_2-Phe Arom $H_{3,5}$: Phe $C_\beta H_2$	3.23	0.26
NH_2-Phe Arom $H_{2,6}$: Phe Arom $H_{3,5}$	3.24	0.26
NH_2-Phe Arom $H_{2,6}$: Phe $C_\beta H_2$	3.37	0.27
NH_2-Phe Arom $H_{2,6}$: Phe Arom $H_{2,6}$	3.50	0.28
NH_2-Phe Arom $H_{3,5}$: Phe $C_\alpha H$	3.60	0.29
NH_2-Phe Arom $H_{2,6}$: Phe $C_\alpha H$	3.68	0.29

[a] Distance used as reference.

and chemical shift anisotropy are responsible for these components being NMR 'silent'.[39,42] Measurements of ^{1}H-NMR peak intensity can give an indication of the concentration of NMR 'silent' *vs.* NMR 'visible' gelator molecules in solution-state NMR spectra. This technique was used to monitor the self-assembly processes of Phe in the presence of NH_2-Phe. The ^{1}H-NMR peaks of Phe and NH_2-Phe became broader and less intense throughout the gelation process of a hot solution of Phe/NH_2-Phe (1 : 0.1) (Fig. 15), consistent with aggregation and formation of solution-state NMR 'silent' components.[42] Interestingly, NH_2-Phe protons showed reduced

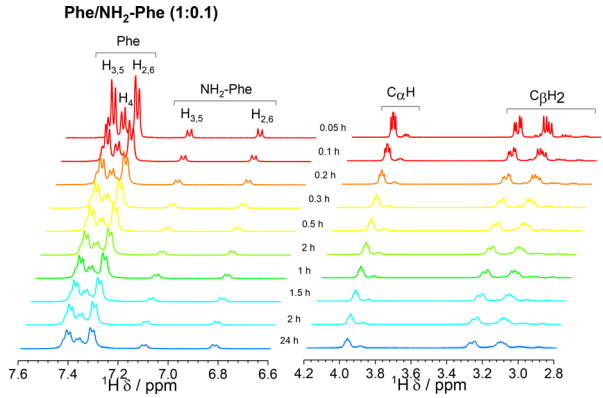

Fig. 15 Kinetics of gelation monitored *via* the acquisition of ^{1}H-NMR spectra over time, immediately after cooling down a hot solution of Phe/NH_2-Phe (1 : 0.1), with gradual formation of a hydrogel. Colour scheme represents the temperature of the solution, as all spectra were acquired at 298 K.

peak intensities, a strong indication that *ca.* 35% of NH_2-Phe molecules were also entrapped in the rigid gel fibres (Table S7†).

As the concentration of NH_2-Phe in the Phe hydrogels was continuously raised, an increased peak intensity for Phe protons was recorded, reflecting the higher concentration of Phe dissolved in solution (Fig. 16 and Table S7†). Sharp and intense ^{1}H peaks revealed the molecular variations associated with the formation

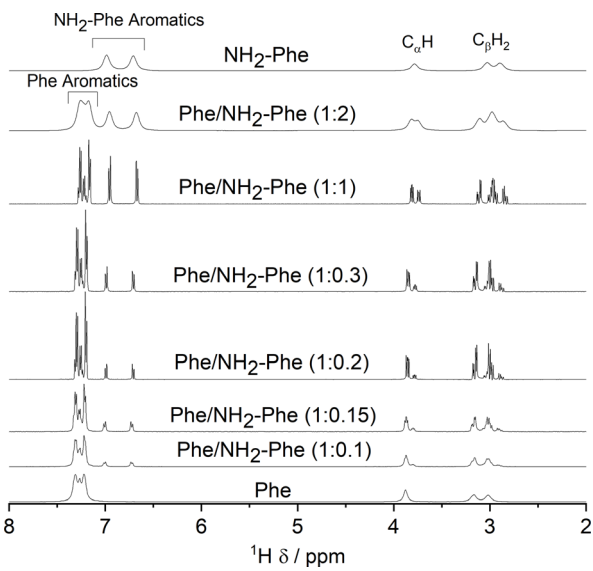

Fig. 16 ^{1}H solution-state NMR spectra of the Phe (303 mM), Phe/NH_2-Phe (1 : 0.1), Phe/NH_2-Phe (1 : 0.15), Phe/NH_2-Phe (1 : 0.2), Phe/NH_2-Phe (1 : 2) and NH_2-Phe (606 mM) hydrogels, Phe/NH_2-Phe (1 : 0.3) suspension and Phe/NH_2-Phe (1 : 1) solution, acquired at 298 K.

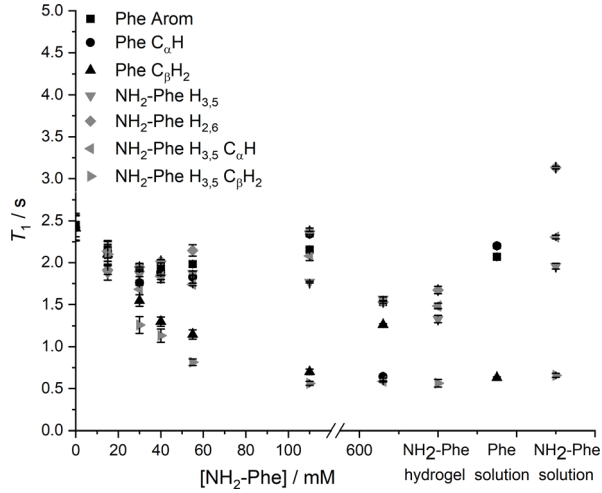

Fig. 17 ^{1}H solution-state longitudinal relaxation times (T_1) of Phe (303 mM) hydrogels with variable concentration of NH_2-Phe, NH_2-Phe (606 mM) hydrogel, and Phe (100 mM) and NH_2-Phe (100 mM) solutions.

of a suspension at Phe/NH_2-Phe (1 : 0.3), exhibiting spectral features characteristic of isotropic solutions. It was concluded that the co-existence of Phe and NH_2-Phe (at these molar ratios and concentrations) increased their water solubilities and led to disruption of the supramolecular network.

Since relaxation processes are affected by ^{1}H mobilities, these could be used to probe molecular motions in supramolecular gels.[38] ^{1}H longitudinal relaxation times (T_1) were monitored throughout the gel-to-solution transitions of these thermoreversible materials. The ^{1}H T_1 times were similar for different ^{1}H species in the Phe hydrogel (Fig. 17), a behaviour associated with fast exchange processes occurring between gel and solution states.[37] The resulting ^{1}H T_1 values are an average of molecules in both environments.[37,38]

When low concentrations of NH_2-Phe were added to the Phe hydrogel, the ^{1}H T_1 times were similar for different ^{1}H sites of NH_2-Phe (Fig. 17). The similarity of the ^{1}H T_1 values proved that Phe and NH_2-Phe were exchanging between gel and solution states, a phenomenon reported previously by our group.[37] After the addition of 40 mM of NH_2-Phe (molar ratio of 1 : 0.15), the similarity between T_1 values for different groups was lost. A full distribution of T_1 times, typical of solutions, was observed when the concentration of NH_2-Phe was over 55 mM (molar ratio of 1 : 0.2). Above this concentration, the system was dominantly composed of fast-tumbling molecules of Phe and NH_2-Phe dissolved in isotropic pools of solvent, a consequence of the destruction of the supramolecular network, in agreement with the sharp and intense peaks detected in the corresponding ^{1}H spectrum (Fig. 16).

Similarly, the ^{1}H T_1 times in pure NH_2-Phe and mixed Phe/NH_2-Phe hydrogels presented a dispersion of values in the gel state similar to solutions of NH_2-Phe, contrasting with the pure Phe hydrogel (Fig. 17). The linear dependence of ^{1}H T_1 times on temperature (Fig. S17†) pointed towards Phe and NH_2-Phe being mainly dissolved throughout the range of temperatures. These results reflected different

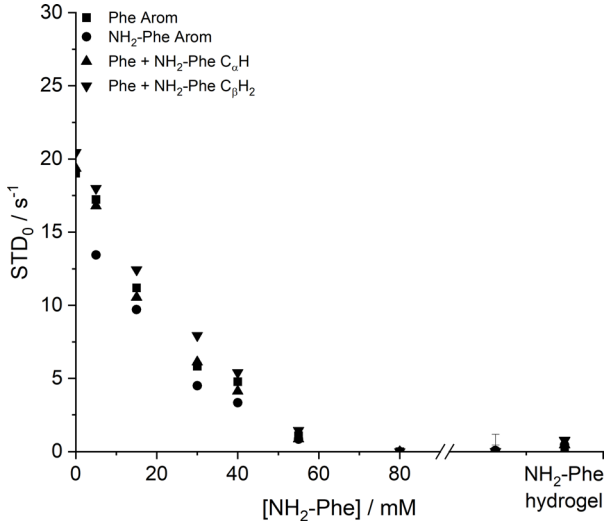

Fig. 18 Initial slope of build-up curves (STD_0) of Phe hydrogels with increasing concentrations of NH_2-Phe, measured at 298 K.

dynamics of exchange of molecules between gel and solution environments for the pure NH_2-Phe gel and mixed gels when compared with the pure Phe gel material.

Saturation transfer difference (STD) NMR experiments were carried out to assess the dynamics of exchange at the gel/solution interfaces.[37,42,43] A mono-exponential evolution of build-up of saturation in solution was observed for the Phe hydrogel (Fig. 18), indicative of fast exchange phenomena between gel and solution states on the NMR relaxation time scale.[37]

The initial slope for the fractional STD response, STD_0, decreased gradually as higher concentrations of NH_2-Phe were introduced (Fig. 18). More importantly, no build-up of saturation was detected at concentrations of NH_2-Phe higher than 55 mM (molar ratio of 1 : 0.2). Since STD NMR experiments rely on the transfer of saturation from a large supramolecular network, which acts as a reservoir of magnetisation, to protons in close proximity, these studies proved further that the supramolecular network lost its structural integrity at molar ratios higher than Phe/NH_2-Phe (1 : 0.2). This was in agreement with ^{1}H longitudinal relaxation findings and was consistent with the loss of self-sustaining properties macroscopically observed. These experiments allowed determination of the 'breaking point' of the network at the molecular level.

Low initial build-up values (STD_0) were observed in the pure NH_2-Phe and mixed Phe/NH_2-Phe hydrogels (Fig. 18). Accumulation of saturation in solution for Phe was therefore less efficient in the multiple-gelator hydrogel. When variable-temperature NMR measurements were carried out to investigate exchange phenomena, the levels of accumulation of saturation in solution decreased with temperature (Fig. S8 and S9†), showing that the rate of exchange between bound and free states was increased. This allowed the conclusion that, at room temperature, Phe and NH_2-Phe exchange at the gel/solution interfaces

faster than the NMR relaxation time scale, as a consequence of weak intermolecular interactions.

Summary

Phe self-assembles into organised gels in water.[16] However, hydrogelation of Phe can be prevented when this gelator molecule is mixed with NH_2-Phe at molar ratios between 1 : 0.2 and 1 : 2 (Phe/NH_2-Phe), with either a suspension or solution being formed. Macroscopic observations showed that the hydrogels lost their structural integrity when the ratios of Phe/NH_2-Phe were above 1 : 0.2, but solution-state NMR studies showed this was a continuous process. ^{1}H-NMR and longitudinal relaxation studies indicated there was gradual solubilisation of Phe and NH_2-Phe in water as NH_2-Phe was added, with sharp and intense ^{1}H-NMR peaks being accompanied by a distribution of ^{1}H T_1 times resembling those of solutions, which became more marked above a ratio of 1 : 0.2 (55 mM of NH_2-Phe). Consequently, the considerable dissolution of the network promoted by NH_2-Phe led to the disappearance of the STD NMR response at this concentration, due to the absence of a supramolecular structure capable of accumulating and transferring saturation. When monitoring both disruption and gelation phenomena, it was found that NH_2-Phe was equally involved in pre-gelation aggregation, possibly manifesting its disruption effects in early nucleation processes. This was attributed to the interference of NH_2-Phe with the electrostatic interactions between Phe dimers, as $C_\alpha H$ and $C_\beta H_2$ protons from both molecules exhibited the most significant chemical shift variation and the strongest intermolecular nOe enhancement in 2D ^{1}H–^{1}H NOESY studies. Such intermolecular interactions between Phe and NH_2-Phe increased their water solubilities, explaining the formation of a clear brown solution at a ratio of 1 : 1. This probably results from solution complexation processes, with the formation of a stable and soluble Phe/NH_2-Phe complex in solution.[44]

When working at higher concentrations of NH_2-Phe, a different scenario was encountered. NH_2-Phe was mixed with Phe at gel-forming concentrations ([Phe] > 212 mM and [NH_2-Phe] > 388 mM), and multiple-gelator hydrogels of Phe/NH_2-Phe were obtained. Morphology studies showed the formation of individual fibres of Phe or NH_2-Phe, pointing towards a system that maintains the structure of the pure gelators, a phenomenon named self-sorting. Their supramolecular arrangements seemed to be dominated by the NH_2-Phe crystal structure, as diffraction experiments showed great similarity between the crystalline components of NH_2-Phe and Phe/NH_2-Phe hydrogels. However, investigation of local molecular environments *via* solid-state NMR spectroscopy showed a certain degree of supramolecular disorder. The line broadening observed in ^{1}H–^{13}C CP/MAS NMR spectra and the presence of additional ^{15}N environments for Phe provided evidence that both gelator molecules were differently surrounded within the rigid mixed fibres. Moreover, the dispersion of ^{1}H T_1 values and the low STD NMR response reflected modification of their dynamics of exchange at the gel/solution interfaces in comparison with pure hydrogels. These data provided evidence of interaction between both gelator molecules in solution and on the surface of the mixed hydrogel fibres. It is the affinity of Phe for NH_2-Phe, and *vice versa*, that is behind the presence of both molecules in the solid fibres. We hypothesised that multiple-gelator hydrogels were composed of purely self-sorted

fibres in a delicate balance with co-assembled structures formed of both Phe and NH_2-Phe molecules.

We also found out that NH_2-Phe is able to independently self-assemble in water to give rise to strong brown gels above 388 mM. The three-dimensional ordering of the needle-like crystalline fibres was determined to be an $(NH_2\text{-Phe})_2(H_2O)_3$ structure using diffraction methods, giving a very good agreement with solid-state NMR experiments. These fibres incorporated *ca.* 80% of the gelator molecules, with the rest coexisting dissolved in pools of water or partially trapped at the fibre interfaces, and exchanging between both environments. The dynamics of this exchange were faster than in the pure Phe hydrogel, highlighting the importance of the Phe head group in dictating the strength of intermolecular interactions.[45]

Conclusions

Phe and NH_2-Phe were found to self-assemble in water into crystalline hydrogels, and we managed to determine the crystal structure of the NH_2-Phe gels. The determined faster dynamics of exchange between gel and solution states of NH_2-Phe in comparison with Phe were correlated with weaker intermolecular interactions, highlighting the role of head groups in dictating the strength of intermolecular interactions.

When mixed in water, different products were obtained depending on the concentration and molar ratio of the gelator molecules. At low concentrations of NH_2-Phe, disruption of the network was promoted by interference of the aliphatics of NH_2-Phe with the electrostatic interactions between Phe molecules, which are the anisotropic forces of self-assembly of Phe. The affinity between both molecules in solution, forming a solution complex, most likely is responsible for network disruption and provided clues on their interaction in the solid state. At high concentrations of NH_2-Phe, multiple-gelator hydrogels were formed with crystal habits different from those of the pure gel fibres, as new environments were detected using solid-state NMR. Consequently, in these mixed materials, the interactions between Phe and NH_2-Phe were different from those present in pure hydrogels, and the phenomenon of exchange at the gel/solution interfaces was modulated. Despite Phe and NH_2-Phe forming different crystal structures, their molecular similarity and similar potential to participate in non-covalent bonds allows them to intimately interact in solution during self-assembly processes, which is manifested at larger scales by the modulation of the resulting fibres at gel-forming concentrations. These findings may provide an insight into the mechanisms of prevention of accumulation of Phe, as well as aggregation processes of peptides and proteins in pathological processes.

Experimental section

Materials

Reagent grade (>98%) L-phenylalanine and hexamethylbenzene (HMB) were purchased from Sigma-Aldrich and 4-amino-L-phenylalanine from Fluorochem. L-[^{13}C9,^{15}N]-Phenylalanine and L-[^{15}N]-glycine were purchased from Cortecnet. Deuterium oxide and 4,4-dimethyl-4-silapentane-1-sulfonic acid (DSS) were purchased from Goss Scientific. We note that, in some cases, care should be taken

with commercial samples of 4-amino-L-phenylalanine as these are not always sufficiently pure to ensure that gelation is reproducible. Milli-Q water was obtained with a Thermo Scientific Barnstead Nanopure purification system coupled to a Barnstead hollow fibre filter.

Methods

Sample preparation. Variable concentrations of Phe and NH_2-Phe were mixed with water (1 mL) in a glass vial (2 cm diameter). Dissolution was promoted with a vortex mixer for 30 s, followed by heating the samples to 363 K using a hot plate. After obtaining a clear solution, the samples were immediately quenched in an ice bath with constant agitation. Subsequently, gelation was assessed *via* the vial-inversion test. The samples were left resting overnight at room temperature and analysed 24 hours after preparation. Dried hydrogel samples were prepared under vacuum.

Scanning electron microscopy. The morphology of the gel fibres was determined using scanning electron microscopy. SEM experiments were carried out using a Jeol JSM-5900 LV Oxford instrument operating at an accelerating voltage of 20 kV. Hydrogels were mounted on aluminium stubs with double-sided carbon adhesive and gold coated using a Polaron SC7640 Quorom Technologies gold sputter coater.

Rheology. The resistance of fibres to mechanical stress was investigated using rheometry. The measurements were performed on a Bohlin Gemini HR nano Rotonetic 2 drive equipped with a Julabo F12 water cooler and circulator controlling the temperature of the bottom Peltier plate, and a stainless-steel parallel-plate geometry system (40 mm diameter plate). Hot solutions (*ca.* 1 mL) were pipetted into a 500 μm gap, with the temperature of the plate maintained at 323 K for sample preparation. The temperature was then lowered to 293 K, the system was covered with a solvent trap to prevent solvent evaporation and the hydrogels were left stabilising for 1 h. The phase angle (δ), storage modulus (G') and loss modulus (G'') were monitored and recorded as a function of frequency and stress. All samples were subjected to frequency sweeps in the range of 0.1 to 100 Hz and an applied stress of 500 Pa, as well as stress amplitude sweeps in the range of 1 to 7000 Pa.

Single-crystal X-ray diffraction. The crystallographic details of the fibre-shaped crystals are:

Crystal data for $(NH_2\text{-Phe})_2(H_2O)_3$: $C_{18}\,H_{30}\,N_4\,O_7$, M = 414.46, clear colourless needle, 0.40 × 0.05 × 0.01 mm^3, monoclinic, space group $P2_1$ (No. 4), a = 5.9813(9) Å, b = 11.3702(15) Å, c = 14.985(2) Å, β = 93.681(8)°, V = 1017.0(2) $Å^3$, Z = 2, D_c = 1.353 g cm^{-3}, F_{000} = 444, Bruker APEX-II CCD, MoKα radiation, λ = 0.71073 Å, T = 100.15 K, $2\theta_{max}$ = 51.6°, 2591 reflections collected, 2591 unique (R_{int} (merged) = 0.0726). Final GooF = 1.086, R_1 = 0.0573, wR_2 = 0.1576, R indices based on 2295 reflections with $I > 3s(I)$ (refinement on F^2), 277 parameters, 15 restraints. Lp and absorption corrections applied, μ = 0.105 mm^{-1}.

Powder X-ray diffraction. The long-range order of these materials was investigated using powder X-ray diffraction. PXRD experiments were performed using a Thermo Scientific ARL XTRA powder diffractrometer and analysed under Cu Kα radiation (λ = 1.54 nm) in the range of 3 to 36° 2θ, using a step size of 0.01° 2θ and a scan time of 6 s. Hydrogels (*ca.* 1 mL) or dried hydrogel samples were transferred

onto a stainless-steel sample holder and analysed immediately to prevent dehydration.

Nuclear magnetic resonance spectroscopy

Solid-state NMR spectroscopy. Solid-state NMR experiments were performed using a Bruker Avance III spectrometer at a ^{1}H frequency of 400.23 MHz, ^{13}C frequency of 100.65 MHz and ^{15}N frequency of 40.56 MHz, equipped with a 4 mm triple resonance wide-bore probe. 40 μL hot solutions were transferred into Kel-F inserts and allowed to cool down to room temperature, after which gels were obtained. ^{1}H–^{13}C CP/MAS NMR experiments were conducted using a recycle delay of 20 s and a contact time of 2 ms. ^{1}H–^{13}C CP/MAS NMR spectra of reference solid powders, dried gel samples and hydrogels were acquired using 128, 2048 or 8192 scans, respectively. A magic-angle spinning (MAS) rate of 10 kHz was used for dried powder and gel samples and a rate of 8.5 kHz was used for hydrogels. ^{1}H–^{15}N CP/MAS experiments were conducted using 4096 scans, a recycle delay of 10 s and a contact time of 2 ms. An MAS rate of 10 kHz was used for dried gel samples and a rate of 8.5 kHz was used for hydrogels. High-field solid-state NMR experiments were carried out using a Bruker Avance III NMR spectrometer operating at a ^{1}H frequency of 850.22 MHz, ^{13}C frequency of 231.81 MHz and ^{15}N frequency of 86.15 MHz, equipped with a 3.2 mm triple resonance probe. Dried samples were packed directly into 3.2 mm zirconia rotors. ^{1}H–^{15}N CP/MAS spectra were acquired using 1024 scans, a recycle delay of 10 s, a contact time of 2 ms and an MAS rate of 10 kHz. ^{1}H and ^{13}C spectra were referenced to tetramethylsilane (TMS). ^{15}N spectra were referenced to liquid NH_3. Hartmann-Hahn conditions were matched using hexamethylbenzene (HMB) for ^{1}H–^{13}C experiments and L-[^{15}N]-glycine for ^{1}H–^{15}N experiments. All experiments were conducted at 298 K.

Solution-state NMR spectroscopy. Solution-state NMR experiments were performed using a Bruker Avance I spectrometer at a ^{1}H frequency of 499.69 MHz equipped with a 5 mm probe. 600 μL hot solutions were transferred into NMR tubes and allowed to cool down to room temperature, after which gels were obtained. Variable temperature (VT) experiments were carried out from 278 to 353 K, allowing thermal stabilisation of the sample for 15 min. 4,4-dimethyl-4-silapentane-1-sulfonic acid (DSS) was used as an internal NMR standard inside a coaxial insert.

^{1}H-NMR spectra were acquired with excitation sculpting for water suppression (zgespg), a recycle delay of 10 s and 16 scans. ^{1}H longitudinal relaxation times (T_1) were measured using a standard inversion recovery pulse sequence with a recycle delay of 10 s and 8 scans. 16 points were recorded at variable time delays ranging from 0.1 to 20 s. The evolution of intensities was fitted mathematically to the mono-exponential function $M_z(\tau) = M_0 \times \left[1 - e^{\left(\frac{-\tau}{T_1}\right)}\right]$, where M_z is the z-component of magnetisation, M_0 is the equilibrium magnetisation and τ is the time delay.[46]

2D ^{1}H–^{1}H Nuclear Overhauser effect spectroscopy (NOESY) experiments were recorded using a phase-sensitive 2D NOESY pulse sequence with WATERGATE for water suppression (noesygppph19). 16 points were recorded using variable mixing times (τ_m = 0.01, 0.1, 0.25 and 0.5), a recycle delay of 2 s and 32 scans. Internuclear distances were calculated according to the Initial Rate Approximation,

which establishes that the initial build-up of NOE enhancements with mixing time is approximately linear. The cross-relaxation rate could therefore be determined from the initial slope of the build-up curve (I_{IS} as a function of t_m), where the NOE enhancement (I_{IS}) was defined as the ratio between the intensity of the cross-peak and the intensity of the sum of the diagonal peaks, an approach that has been applied to organogels by Canet *et al.* (2012).[39] In turn, the cross-relaxation rate (s_{IS}) was proportional to the inverse sixth power of the internuclear distance,

$$s_{IS} = \zeta r_{IS}^{-6}. \quad (1)$$

This relationship between intensity and distance allowed the observed nOe intensities to be calibrated relative to a known internuclear distance (NH_2-Phe $H_{2,6}$ – NH_2-Phe $H_{3,5}$) within the supramolecular system.[39,47,48]

Saturation transfer difference NMR experiments were performed with selective saturation of a determined ^{1}H frequency using a train of 40 Gaussian pulses with a duration of 50 ms (stddiffgp19.2), acquired with a recycle delay of 6 s and 16 scans. STD spectra were created by the subtraction of an on-resonance spectrum (STD_{on}), in which a spectral region was selectively saturated, to an off-resonance spectrum (STD_{off}), acquired with no selective saturation. Interleaved acquisition of STD_{on} and STD_{off} spectra was performed as pseudo-2D experiments to minimise artefacts caused by variations throughout the experiment. STD_{on} spectra were acquired at a saturation frequency of 1 ppm (where only resonances of the network could be encountered), whereas the STD_{off} saturation frequency was set to 40 ppm. Each pair of experiments was carried out at variable saturation times ranging from 0.25 to 6 s. The signal intensity in the STD spectrum relative to the STD_{off} spectrum was used to determine the fractional STD response, η_{STD}:

$$\eta_{STD} = \frac{I_0 - I_{SAT}}{I_0} \times 100 = \frac{I_{STD}}{I_0} \times 100 \quad (2)$$

where I_0 is the signal intensity from the STD_{off} spectrum, I_{SAT} is the signal intensity from the STD_{on} spectrum and I_{STD} is the signal intensity from the difference spectrum.[49] STD build-up curves were fitted mathematically to the mono-exponential function $STD_{(t_{sat})} = STD^{max}\,(1 - e^{(-k_{sat}\cdot t_{sat})})$, from which initial slope values, STD_0, were obtained from the product $STD^{max} \times k_{sat}$. k_{sat} is the saturation rate constant and t_{sat} is the saturation time.

Author contributions

Susana M. Ramalhete: conceptualization, formal analysis, investigation, writing – original draft, review and editing, visualization, funding acquisition; Karol P. Nartowski: conceptualization, methodology, investigation, writing – original draft, review and editing; Hayley Green: analysis, investigation, writing – review and editing; Jesús Angulo: analysis, conceptualization, methodology, investigation, writing – review & editing, supervision; Dinu Iuga: analysis, investigation, writing – review and editing; László Fábián: analysis, conceptualization, methodology, investigation, writing – review and editing, supervision; Gareth O. Lloyd: analysis, conceptualization, methodology, investigation, writing – review and

editing, supervision, funding acquisition; Yaroslav Z. Khimyak: analysis, conceptualization, methodology, investigation, writing – original draft, review and editing, supervision, funding acquisition.

Conflicts of interest

There are no conflicts of interest to declare.

Acknowledgements

The UK 850 MHz solid-state NMR Facility used in this research was funded by the EPSRC and BBSRC (contract reference PR140003), as well as the University of Warwick including *via* part funding through Birmingham Science City Advanced Materials Projects 1 and 2 supported by Advantage West Midlands (AWM) and the European Regional Development Fund (ERDF). SMR also thanks Mr B. Lézé for conduction of SEM and PXRD measurements. SMR thanks the University of East Anglia for the postgraduate studentship. GOL thanks the Heriot-Watt University and the Royal Society of Edinburgh/Scottish Government Personal Research Fellowship scheme for funding. GOL and YZK are grateful to EPSRC Directed Assembly Network for financial support. We acknowledge the use of the 850 MHz solid-state NMR facility at the University of Warwick for the high-field and very fast MAS NMR experiments.

References

1 J. W. Steed, Supramolecular gel chemistry: developments over the last decade, *Chem. Commun.*, 2011, **47**(5), 1379–1383.
2 D. J. Adams, Dipeptide and Tripeptide Conjugates as Low-Molecular-Weight Hydrogelators, *Macromol. Biosci.*, 2011, **11**(2), 160–173.
3 D. K. Kumar and J. W. Steed, Supramolecular gel phase crystallization: orthogonal self-assembly under non-equilibrium conditions, *Chem. Soc. Rev.*, 2014, **43**(7), 2080–2088.
4 N. Peppas, P. Bures, W. Leobandung and H. Ichikawa, Hydrogels in pharmaceutical formulations, *Eur. J. Pharm. Biopharm.*, 2000, **50**(1), 27–46.
5 R. Fairman and K. S. Åkerfeldt, Peptides as novel smart materials, *Curr. Opin. Struct. Biol.*, 2005, **15**(4), 453–463.
6 K. J. Skilling, F. Citossi, T. D. Bradshaw, M. Ashford, B. Kellam and M. Marlow, Insights into low molecular mass organic gelators: a focus on drug delivery and tissue engineering applications, *Soft Matter*, 2014, **10**(2), 237–256.
7 V. Jayawarna, M. Ali, T. A. Jowitt, A. F. Miller, A. Saiani, J. E. Gough, *et al.*, Nanostructured hydrogels for three-dimensional cell culture through self-assembly of fluorenylmethoxycarbonyl–dipeptides, *Adv. Mater.*, 2006, **18**(5), 611–614.
8 H. Wang, L. Lv, G. Xu, C. Yang, J. Sun and Z. Yang, Molecular hydrogelators consist of Taxol and short peptides/amino acids, *J. Mater. Chem.*, 2012, **22**(33), 16933–16938.
9 L. E. Buerkle and S. J. Rowan, Supramolecular gels formed from multi-component low molecular weight species, *Chem. Soc. Rev.*, 2012, **41**(18), 6089–6102.

10 A. R. Hirst and D. K. Smith, Two-Component Gel-Phase Materials—Highly Tunable Self-Assembling Systems, *Chem.–Eur. J.*, 2005, **11**(19), 5496–5508.
11 L. Adler-Abramovich, L. Vaks, O. Carny, D. Trudler, A. Magno, A. Caflisch, *et al.*, Phenylalanine assembly into toxic fibrils suggests amyloid etiology in phenylketonuria, *Nat. Chem. Biol.*, 2012, **8**(8), 701–706.
12 T. D. Do, W. M. Kincannon and M. T. Bowers, Phenylalanine oligomers and fibrils: the mechanism of assembly and the importance of tetramers and counterions, *J. Am. Chem. Soc.*, 2015, **137**(32), 10080–10083.
13 S. Shaham-Niv, A. Ezra, D. Zaguri, S. R. Shotan, E. Haimov, H. Engel, *et al.*, Targeting phenylalanine assemblies as a prospective disease-modifying therapy for phenylketonuria, *Biophys. Chem.*, 2024, **308**, 107215.
14 W.-P. Hsu, K.-K. Koo and A. S. Myerson, The gel-crystallization of 1-phenylalanine and aspartame from aqueous solutions, *Chem. Eng. Commun.*, 2002, **189**(8), 1079–1090.
15 V. Singh, R. K. Rai, A. Arora, N. Sinha and A. K. Thakur, Therapeutic implication of L-phenylalanine aggregation mechanism and its modulation by D-phenylalanine in phenylketonuria, *Sci. Rep.*, 2014, **4**, 3875.
16 K. P. Nartowski, S. M. Ramalhete, P. C. Martin, J. S. Foster, M. Heinrich, M. D. Eddleston, *et al.*, The Plot Thickens, Gelation by Phenylalanine in Water and Dimethyl Sulfoxide, *Cryst. Growth Des.*, 2017, **17**, 4100–4109.
17 H. M. Wyss, Rheology of soft materials, *Fluids, Colloids, and Soft Materials: An Introduction to Soft Matter Physics*, 2016, vol. 7, p. 149.
18 F. M. Menger and K. L. Caran, Anatomy of a gel. Amino acid derivatives that rigidify water at submillimolar concentrations, *J. Am. Chem. Soc.*, 2000, **122**(47), 11679–11691.
19 M. Lusi, Solid solutions mixed crystals and eutectics, in *Comprehensive Supramolecular Chemistry II*, 2017, 109–125.
20 E. Schur, E. Nauha, M. Lusi and J. Bernstein, Kitaigorodsky revisited: polymorphism and mixed crystals of acridine/phenazine, *Chem.–Eur. J.*, 2015, **21**(4), 1735–1742.
21 A. J. Cruz-Cabeza, M. Lestari and M. Lusi, Cocrystals Help Break the "Rules" of Isostructurality: Solid Solutions and Polymorphism in the Malic/Tartaric Acid System, *Cryst. Growth Des.*, 2018, **18**(2), 855–863.
22 Y. Yang, H. Zhang, S. Du, M. Chen, S. Xu, L. Jia, *et al.*, Ternary phase diagram and the formation mechanism of two distinct solid solutions of amino acid systems: L-Valine/L-norvaline and L-valine/L-alanine, *J. Chem. Thermodyn.*, 2018, **119**, 34–43.
23 E. Nauha, P. Naumov and M. Lusi, Fine-tuning of a thermosalient phase transition by solid solutions, *CrystEngComm*, 2016, **18**(25), 4699–4703.
24 O. Shemchuk, D. Braga and F. Grepioni, Alloying barbituric and thiobarbituric acids: from solid solutions to a highly stable keto co-crystal form, *Chem. Commun.*, 2016, **52**(79), 11815–11818.
25 M. Lusi, I. J. Vitorica-Yrezabal and M. J. Zaworotko, Expanding the scope of molecular mixed crystals enabled by three component solid solutions, *Cryst. Growth Des.*, 2015, **15**(8), 4098–4103.
26 C. F. Mackenzie, P. R. Spackman, D. Jayatilaka and M. A. Spackman, CrystalExplorer model energies and energy frameworks: extension to metal coordination compounds, organic salts, solvates and open-shell systems, *IUCrJ*, 2017, **4**(5), 575–587.

27 D. E. Braun and U. J. Griesser, Supramolecular organization of nonstoichiometric drug hydrates: dapsone, *Front. Chem.*, 2018, **6**, 31.
28 C. Wang and C. C. Sun, Identifying slip planes in organic polymorphs by combined energy framework calculations and topology analysis, *Cryst. Growth Des.*, 2018, **18**(3), 1909–1916.
29 D. Dey, S. Bhandary, S. P. Thomas, M. A. Spackman and D. Chopra, Energy frameworks and a topological analysis of the supramolecular features in in situ cryocrystallized liquids: tuning the weak interaction landscape via fluorination, *Phys. Chem. Chem. Phys.*, 2016, **18**(46), 31811–31820.
30 R. Roy, J. Deb, S. S. Jana and P. Dastidar, Exploiting Supramolecular Synthons in Designing Gelators Derived from Multiple Drugs, *Chem.–Eur. J.*, 2014, **20**(47), 15320–15324.
31 P. Sahoo, N. Adarsh, G. E. Chacko, S. R. Raghavan, V. G. Puranik and P. Dastidar, Combinatorial Library of Primaryalkylammonium Dicarboxylate Gelators: A Supramolecular Synthon Approach, *Langmuir*, 2009, **25**(15), 8742–8750.
32 L. A. Estroff and A. D. Hamilton, Water gelation by small organic molecules, *Chem. Rev.*, 2004, **104**(3), 1201–1218.
33 L. Meazza, J. A. Foster, K. Fucke, P. Metrangolo, G. Resnati and J. W. Steed, Halogen-bonding-triggered supramolecular gel formation, *Nat. Chem.*, 2013, **5**(1), 42–47.
34 W. Kolodziejski and J. Klinowski, Kinetics of cross-polarization in solid-state NMR: a guide for chemists, *Chem. Rev.*, 2002, **102**(3), 613–628.
35 G. J. Martin, M. L. Martin and J.-P. Gouesnard, *15N-NMR Spectroscopy*, Springer Science & Business Media, 2012.
36 D. J. Adams, K. Morris, L. Chen, L. C. Serpell, J. Bacsa and G. M. Day, The delicate balance between gelation and crystallisation: structural and computational investigations, *Soft Matter*, 2010, **6**(17), 4144–4156.
37 S. M. Ramalhete, K. P. Nartwoski, N. Sarathchandra, J. S. Foster, A. N. Round, J. Angulo, *et al.*, Supramolecular amino acid based hydrogels: probing the contribution of additive molecules using NMR spectroscopy, *Chem.–Eur. J.*, 2017, **23**, 8014–8024.
38 C. L. Cooper, T. Cosgrove, J. S. van Duijneveldt, M. Murray and S. W. Prescott, The use of solvent relaxation NMR to study colloidal suspensions, *Soft Matter*, 2013, **9**(30), 7211–7228.
39 S. Bouguet-Bonnet, M. Yemloul and D. Canet, New Application of Proton Nuclear Spin Relaxation Unraveling the Intermolecular Structural Features of Low-Molecular-Weight Organogel Fibers, *J. Am. Chem. Soc.*, 2012, **134**(25), 10621–10627.
40 F. Piana, D. H. Case, S. M. Ramalhete, G. Pileio, M. Facciotti, G. M. Day, *et al.*, Substituent interference on supramolecular assembly in urea gelators: synthesis, structure prediction and NMR, *Soft Matter*, 2016, **12**(17), 4034–4043.
41 G. Clore and A. Gronenborn, Theory and applications of the transferred nuclear Overhauser effect to the study of the conformations of small ligands bound to proteins, *J. Magn. Reson.*, 1982, **48**(3), 402–417.
42 B. Escuder, M. LLusar and J. F. Miravet, Insight on the NMR study of supramolecular gels and its application to monitor molecular recognition on self-assembled fibers, *J. Org. Chem.*, 2006, **71**(20), 7747–7752.

43 M. D. Segarra-Maset, B. Escuder and J. F. Miravet, Selective Interaction of Dopamine with the Self-Assembled Fibrillar Network of a Molecular Hydrogel Revealed by STD-NMR, *Chem.–Eur. J.*, 2015, **21**(40), 13925–13929.
44 A. Jawor-Baczynska, B. D. Moore, H. S. Lee, A. V. McCormick and J. Sefcik, Population and size distribution of solute-rich mesospecies within mesostructured aqueous amino acid solutions, *Faraday Discuss.*, 2013, **167**, 425–440.
45 S. Ramalhete, J. S. Foster, H. R. Green, K. P. Nartowski, M. Heinrich, P. Martin, *et al.*, FDHALO17: Halogen effects on the solid-state packing of phenylalanine derivatives and the resultant gelation properties, *Faraday Discuss.*, 2017, **203**, 423–439.
46 R. R. Ernst, G. Bodenhausen and A. Wokaun, *Principles of Nuclear Magnetic Resonance in One and Two Dimensions*, Clarendon Press Oxford, 1987.
47 C. P. Butts, C. R. Jones, E. C. Towers, J. L. Flynn, L. Appleby and N. J. Barron, Interproton distance determinations by NOE–surprising accuracy and precision in a rigid organic molecule, *Org. Biomol. Chem.*, 2011, **9**(1), 177–184.
48 D. Neuhaus and M. P. Williamson, *The Nuclear Overhauser Effect in Structural and Conformational Analysis*, VCH, New York, 1989.
49 A. Viegas, J. Manso, F. L. Nobrega and E. J. Cabrita, Saturation-transfer difference (STD) NMR: a simple and fast method for ligand screening and characterization of protein binding, *J. Chem. Educ.*, 2011, **88**(7), 990–994.